Morphological, Structural and Chemical Properties of p- type Porous Silicon Produced by Electrochemical Etching

Raid A. Ismail [1,*] *, Nadir F. Habubi* [2] *and Ahmed N. Abd* [3]

[1] Department of Applied Sciences, University of Technology, Baghdad, Iraq

[2] Physics Department, Education Faculty, University of Al- Mustansiriyah, Baghdad, Iraq

[3] Physics Department, Science Faculty, University of Al- Mustansiriyah, Baghdad, Iraq

[*] E-mail: raidismail@yahoo.com

Abstract: In this paper, the nanocrystalline porous silicon (PS) films are prepared by electrochemical etching of p-type silicon wafer with current density (7 mA/cm^2) and etching times on the formation nano-sized pore array with a dimension of around different etching time. The films were characterized by the measurement of XRD, FTIR spectroscopy and atomic force microscopy properties (AFM). We have estimated crystallites size from X-Ray diffraction about nanoscale for porous silicon and Atomic Force microscopy confirms the nanometric size Chemical fictionalization during the electrochemical etching show on the surface chemical composition of PS. The etching possesses inhomogeneous microstructures that contain a-Si clusters (Si$_3$–Si–H) dispersed in amorphous silica matrix . From the FTIR analyses showed that the Si dangling bonds of the as-prepared PS layer have large amount of Hydrogen to form weak Si−H bonds.

The atomic force microscopy investigation shows the rough silicon surface, with increasing etching process (current density and etching time) porous structure nucleates which leads to an increase in the depth and width (diameter) of surface pits. Consequently, the surface roughness also increase.

Keywords: porous silicon; Nanocrystalline porous silicon; Anodization; XRD; FTIR&AFM, porosity.

1   Introduction

Porous silicon (PS) can be defined as a semiconductor material resulting from the electrochemical attack of a strong acid (usually hydrofluoric acid, HF), to form a network of pores with typical diameters ranging from a few nanometers. Sometimes this material is referred to be a quantum sponge[1,2]. The high surface-to-volume ratio (typically in the order of 500 m^2/cm^3), and their inherent electronic and transport characteristics make this material suitable for development of photonic and sensing devices [3]. Although the attention focus driven by PS started in 1990, some previous works have to be mentioned here. Early works on electrochemical treatment of silicon surfaces dealt with problems of anodic   oxidation,   electropolishing   and

chemical etching as early as 1937 (Güntherschulze & Betz, 1937). A more detailed study was performed twenty years later (Schmidt & Michel, 1957)[4]. The first mention of PS material (without being named in that way) was reported in 1956, when A. Uhlir Jr. found unusual deposits on anodized silicon samples (Uhlir, 1956). He

supposed that those deposits corresponded to oxide forms of silicon. Shortly after this, Turner reported a more detailed study of anodically formed films on silicon (Turner, 1958). Years later, in 1971[5], Watanabe and Sakai reported for the first time that the electrochemically formed films on silicon surfaces corresponded to a porous nature (Watanabe & Sakai, 1971). Theunissen modelled the "formation of etch channels which propagate in crystal-oriented directions in the monocrystal" of n-type silicon the following year (Theunissen, 1972). Subsequently, interest on porous silicon began to grow slowly, and important articles dealing with different aspects of the material were published[6].

2   Experimental
2-1   Morphological of porous silicon

Crystalline wafer of p-type Silicon with resistivity of (2-20) Ω.cm, 508 μm thickness, and (100) orientation were used as starting substrates. The substrates were cut into rectangles with areas of (1.5 $\times$ 1.5cm^2). After chemical treatment, 0.1 μm thick Al layers were deposited, by using an evaporation method, on the backsides of the wafer. Electrochemical etching then performed in a mixture (1:1) HF (40%) - Ethanol (99.99) at room temp-erature by using a (Au) electrode as in Fig (1). Current of 7mA/cm^2 applied for (5-15 min) .The etched area of the sample was (0.785 cm^2).
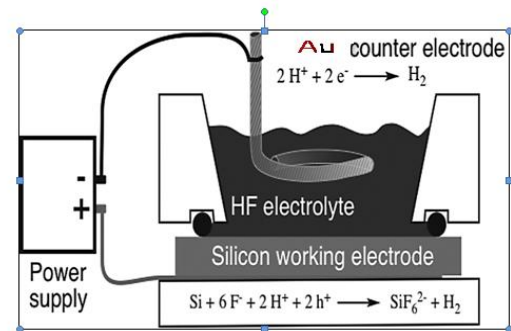

Figure 1 : Cross-sectional view of a lateral anodisation cell [6] .

The morphological properties which include, surface morphology, layer thickness, pore diameter, wall thickness, pore shape, porosity and surface area. These structural properties measured by Atomic

force microscopy Atomic force microscopy (AFM).

2-1-1. porosity "P"

Porosity is defined as the fraction of void within the PS layer and can be determined easily by weight measure-ments. The virgin wafer is first weighed before anodisation (m_1), then just after The higher current causes more solving silicon and anodisation (m_2) and finally after dissolution of the whole porous layer in a molar KOH aqueous solution (m_3)[7]:

$$p (m)\% = (m_1 - m_3) / (m_1 - m_2) \qquad (1)$$

2-1-2. Specific Surface area

A number of properties of material composed of micrometer sized grain, as well as those composed of nanometer-sized articles depend strongly on the surface area .For example, the electrical resistivity of a granular material is expected to scale with the total area of the grain boundaries [8-10].The surface- volume ratio (specific surface area) in m^2/cm^3 could be measured as the following equation Surface Area(S.A.) (m^2/cm^2).

S.A.= Area of one pore × No. of pores /Area of Ps structure ×Depth   **(2)**

The pore geometry was considered as cylindrical in shape and thus the area of one pore is :

The area of one pore = 2π rps × hps.   **(3)**

where rps& hps is the height and radius of pore measured continuously of the pore measured.By taking the maximum value of pore width and the density of the pore was constant before and after oxidation process where it is about $11*10^8$ pore/cm^2.That values was applied in equation (l) we obtained on the surface area values . We can observe that after oxidation the surface area will be decreased that due to, after oxidation porous surface will be saturated and the stable oxygen-Passivated surface will replace unstable Hydrogen-Passivated surface which caused to decrease pore size this will be lead to decrease the surface area [11-12].

2-1-3. surface roughness

3D AFM image of porous silicon in which the irregular and randomly distributed nanocrystalline silicon pillars and voids over the entire surface can be seen. The prepared porous silicon layer shows the surface roughness and pyramid like hillocks surface. Figures show the section analysis of porous structure in which the isolated silicon pillars with steeper sidewalls can be observed which confirms the possibility of achieving quantum confinement effect. The surface morphology confirms the pore formation with its core roughness depth and roughness average[13].

2-1.   Structural 0f porous silicon

X-ray diffraction is the experimental method usually used to evaluate the degree of crystallinity in PS. In addition, high resolution diffraction set up allows a direct determination of the lattice parameters a of the PS layer[14]. X-ray diffraction pattern can clearly display the crystal composition and structure. The Scherer's equation can be exploited to estimate the average grain size D for a knowing X-ray wavelength λ at the diffraction angle θ from the equation as given by [15]:

$$D = K \lambda / FWHM \cos(\theta) \qquad \textbf{(4)}$$

Where the FWHM is the full width at the half maximum of the characteristic spectrum in units of radians, L and λ are in nm .K is the Scherrer constant (1 > K > 0.89).

The peak broadening also depends on the lattice strain induced by mechanical stresses, so that the Williamson-Hall method can be used to improve the analysis [16]. Introducing the component for peak broadening due to lattice strain and rearranging Scherrer equation, we obtain:

FWHM cos θ (Kλ/d) = η sin θ   **(5)**

Where the coefficient η represents the lattice strain. By plotting the term FWHM cosθ values for each peak vs. sinθ and applying a linear fit, crystallites size d can be obtained from y-intercept, In this case, only a mean value of the crystallite dimension can be obtained, which is an average between all the diffraction peaks generated by the nanopowders[17].

2-2.   Chemical Composition of PS Layer

Surface chemical composition of PS is best probed with Fourier Transform Infrared (FTIR) spectroscopy. FTIR signal in PS is larger and easier to measure than in bulk Si due to much larger specific area. The pore surface includes a high density of dangling bonds of Si for original impurities such as hydrogen and fluorine, which are residuals from the electrolyte. Additionally, if the manufactured PS layer is stored in ambient air for a few hours, the surface oxidizes spontaneously[17].

3   Results and Discussion

2D and 3D Atomic force microscopy (AFM) images of the as-anodized porous silicon surface structure formed on p-type for different time etching (5-15 min) are shown in the following figures ,The PS layer

thickness and roughness are not monotonically proportional to the anodization time. The surface morphology measured by AFM is given in figures(2-6), which show that the surface of the PS layer consists of homogeneous and large number of irregularly shaped distributed randomly over the entire surface. Representative (500nm x 500nm).
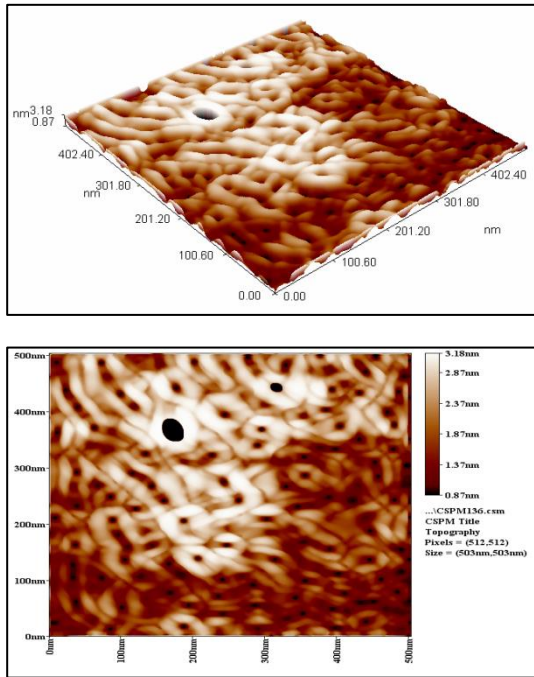

Figure 2:   3D & 2D AFM images (0.5 × 0.5 µm) of porous silicon samples prepared with etching time of (5min) at current density of 7 mA/cm².
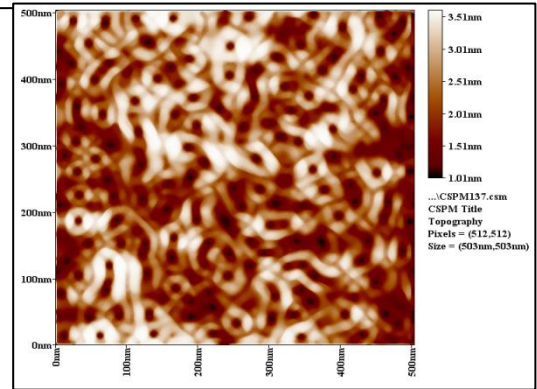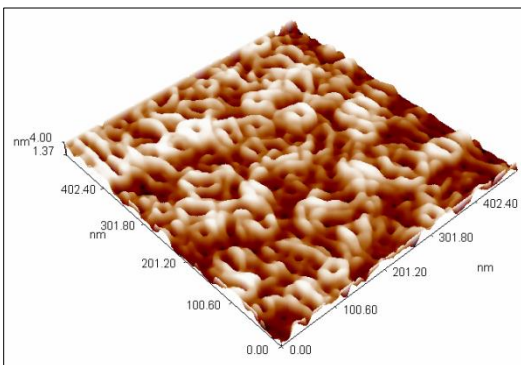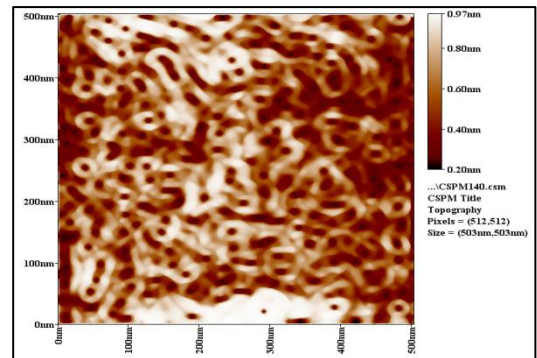

Figure 3: 3D & 2D AFM images (0.5 × 0.5 µm) of porous silicon samples prepared with etching time of (7min) at current density of 7 mA/cm².
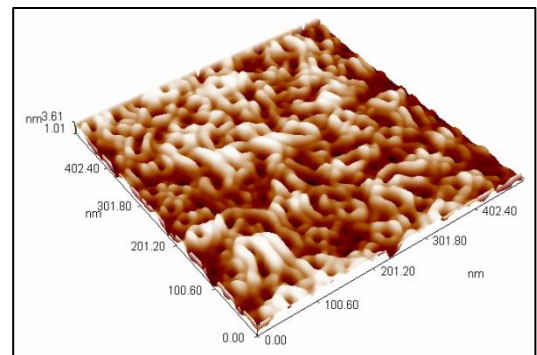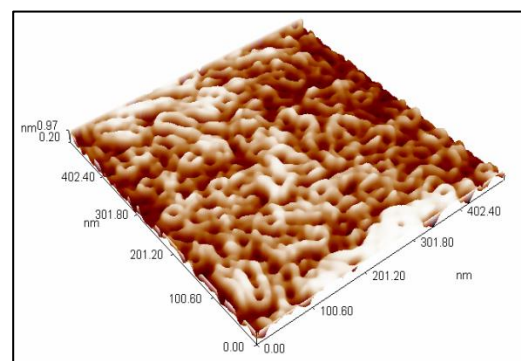

Figure 4 : 2D& 3D AFM images (0.5 × 0.5 µm) of porous silicon samples prepared with etching time of (10 min) at current density of 7 mA/cm².
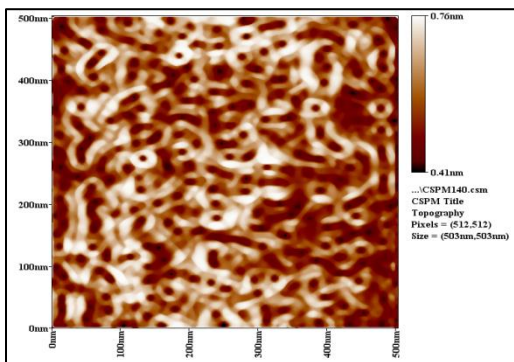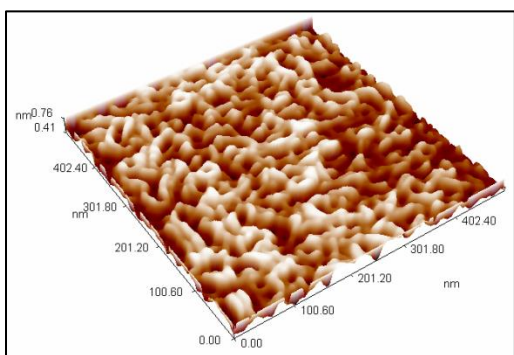
Figure 5: 2D& 3D AFM images (0.5 × 0.5 µm) of porous silicon samples prepared with etching time of (12 min) at current density of 7 mA/cm².

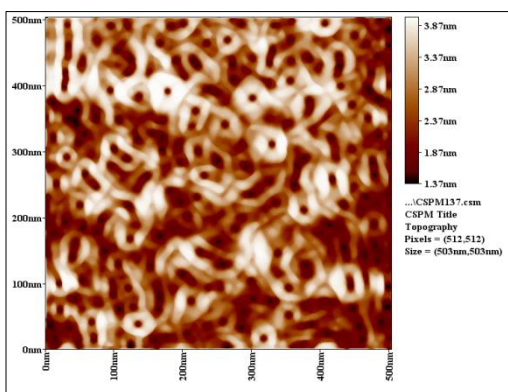*Figure 6 : 2D& 3D AFM images (0.5 × 0.5 µm) of porous silicon samples prepared with etching time of (15 min) at current density of 7 mA/cm²*

The pore diameter and wall size estimated based on the AFM image, from figures we can see that the pore average diameter (16.28 , 19.47 ,24.10 , 21.48 & 22.70 nm) and average wall size (0.84% ,3.88% ,11.59% ,13.5% &22%) were increased with increasing oxidation time,

the increasing in pore diameter due to growth oxide layer within pore lead to replace unstable hydrogen and oxygen by stable and pure oxygen which appears like cloudy covered PS layer. Porosity is estimated by the gravitation method by using equation (1)
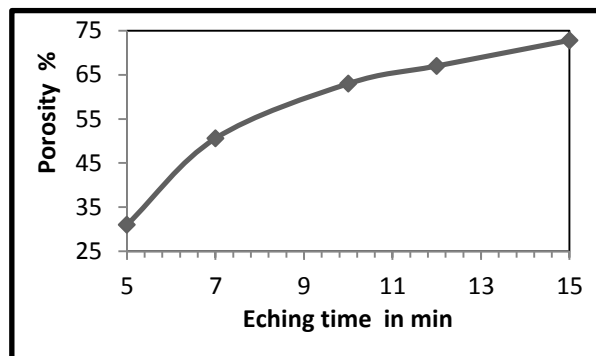

Figure 7: Porosity calculated from AFM porosity measured from gravimetric technique.

X-ray diffraction spectra show a distinct variation between the fresh silicon surface and the porous silicon surfaces formed at different etching times. A strong peak of (p-Si) in 5min eatching time shows a very sharp peak at $2\theta = 69.7°$ oriented only along the (100) direction is observed confirming the monocrystalline structure of the Si layer which belongs to the (100) reflecting plane of Si of cubic structure (according to ICDD N 1997and 2011 JCPDS) as shown in Table (1). With increasing etching time, this peak becomes very broad with varying full-width at half maximum as shown in figure (8) which confirms the formation of porous structure on the crystalline silicon surface.The broadening in the diffracted peaks is due to the increasing thickness of pore walls, and upward shifts are due to relaxation of strain in the porous structure. XRD spectra show the porous silicon is formations and that the structure is amorphous at high current density.
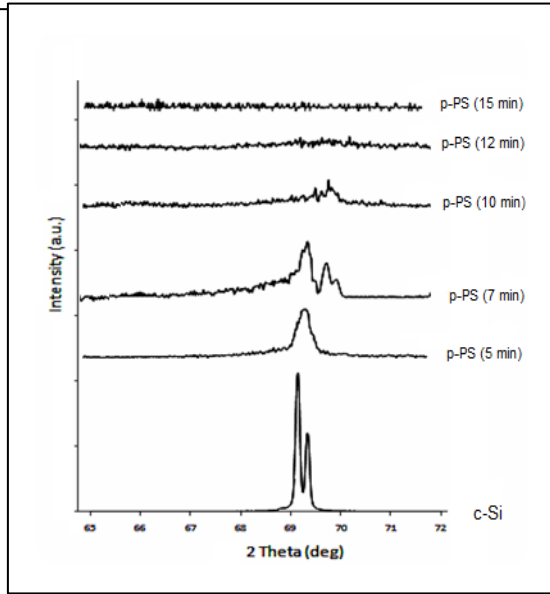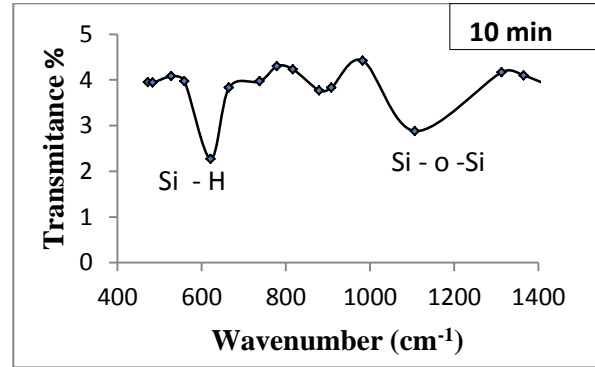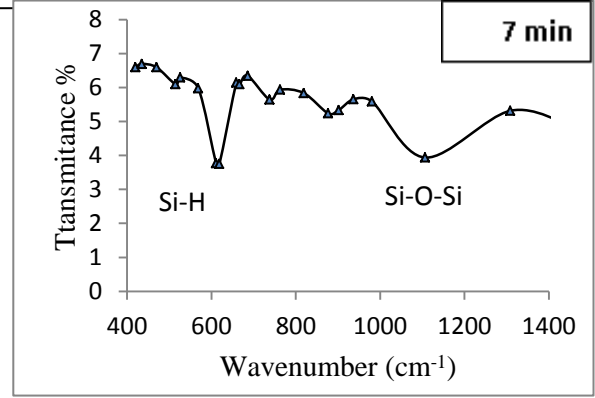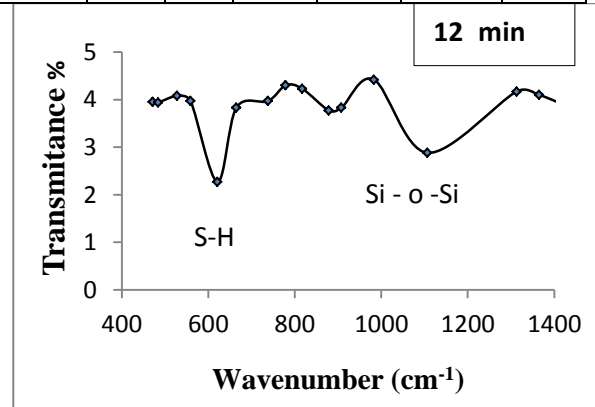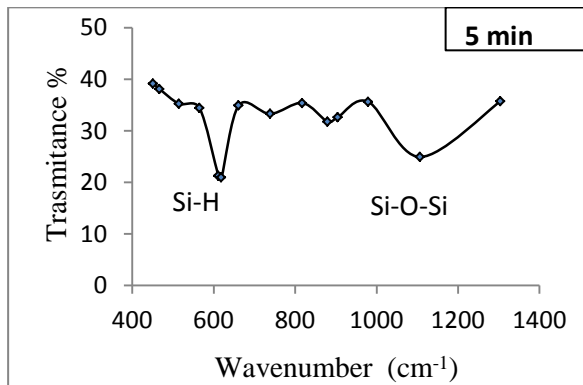
Figure 8 : XRD spectra of PS samples anodized for 7mA/cm², etching current density at (5,7,10,12and 15min) etching time.

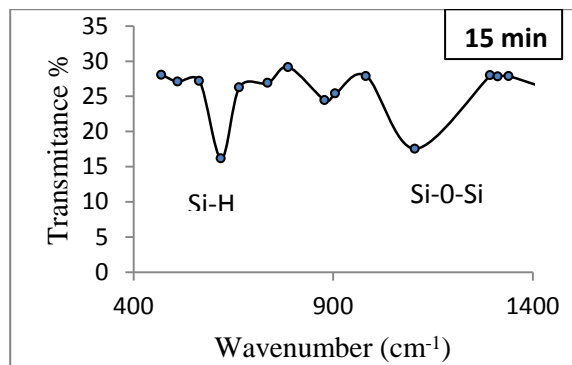*Table 1: Calculated crystalline size, Lattice constant, and strain for p-PS for different etching time.*

The FTIR spectra of the p-type porous silicon are shown in fig (9) , The peaks at around 439.77 cm^{-1} and 1064.71 cm^{-1} are from Si–O–Si stretching modes , which are dependent on the oxidation degree of porous silicon. The transmittance peak at 624.94 cm^{-1} Si-H bending in (Si3-SiH), 871.82 cm^{-1} Si-H$_2$ wagging mode and 910.4 cm^{-1} Si-H$_2$ scissor mode .

Etching time (min)	2theta (deg)	D (A)	FWHM (deg)	D (nm)	Lattice constant (nm)	Strain x10^{-3}
5	69.69	1.34	0.13	74.42	1.348	27.88
7	69.44	1.35	0.16	61.16	1.353	33.93
10	69.12	1.35	0.14	71.43	1.358	29.05
12	69.76	1.34	0.08	126.4	1.347	16.41
15	69.13	1.35	0.09	103.48	1.358	20.05

**Figure 9**: FTIR spectra of the sample p-type oxidized at 300 °C for different etching times.

4 Conclusion

1- The obtained results show that the struct-ural properties of PS layer depend upon the oxidation time , the surface roughness, layer thickness, porosity, and pore diameter are lower than these measured in the lower oxidation time .

2-Samples of porous silicon (PS) were prepared by electrochemical etching meth-od ,their structures were studied with AFM, AFM results were used to calculate the Average Diameter &wall size and ,. The AFM technique doesn't destroy the samples as gravimetric technique. Good correspo-ndent was obtained in results. Optical properties affected

3-The atomic force microscopy investigation shows the rough silicon surface which can be regarded as a condensation point for small skeleton clusters which plays an important role for the characterized the nanocrystalline porous silicon.

4- Porous silicon layers are prepared by electrochemical etching for different current densities and etching times. The samples are then characterized the nanocrystalline porous silicon layer to study its structural, chemical and morphological properties.

5- From the XRD properties we have shown the porous structure and the decrease of the Si nano-sized because a broadening of the Si peaks.

6-In porous silicon, as-prepared samples, oxygen is normally absent, the dominant bonds being Si-H .

References

[1] Xu, Z.P.; Zeng, Q.H.; Lu, G.Q.; Yu, A.B. Inorganic nanoparticles as carriers for efficient cellular delivery. *Chem. Eng. Sci.* 2006, *61*, 1027-1040.

[2] J.H. Park, Gu, L.; von Maltzahn, G.; Ruoslahti, E.; Bhatia, S.N.; Sailor, M.J. Biodegradable luminescent porous silicon nanoparticles for *in vivo* applications. *Nat. Mater.* 2009, *8*, 331-336.

[3] M. Ferrari, Cancer nanotechnology: opportunities and challenges. *Nat. Rev. Cancer* 2005, *5*,161-171.

[4] D.J. Bharali, Khalil, M.; Gurbuz, M.; Simone, T.M.; Mousa, A.S. Nanoparticles and cancer therapy: A concise review with emphasis on dendrimers. *Int. J.Nanomed.* 2009, *4*, 1-7.

[5] U. Popp, Herbig, R.; Michel, G.; Müller, E.; Oestreich. C. Properties of Nanocrystalline Ceramic Powders Prepared by Laser Evaporation and Recondensation. *J. Eur. Ceram. Soc.* 1998, *18*,1153-1160.

[6] P.J Kelly, Arnell, R.D. Magnetron sputtering: a review of recent developments and applications.*Vacuum* 2000, *56*, 159-172.

[7] M.T. Reetz , Helbig, W. Size-Selective Synthesis of Nanostructured Transition Metal Clusters.*J. Am. Chem. Soc.* 1994, *116*, 7401-7402.

[8] B.H., Kear, Strutt, P.R. Chemical processing and applications for nanostructured materials *Nanostruct. Mater.* 1995, *6*, 227-236.

[9] Kusová, K.; Cibulka, O.; Dohnalova, K.; Pelant, I.; Valenta, J.; Fucıkova, A.; Zıdek, K.; Lang, J.; Englich, J.; Matejka, P.; Stepanek, P.; Bakardjieva, S. Brightly Luminescent Organically Capped Silicon Nanocrystals Fabricated at Room Temperature and Atmospheric Pressure. *ACS*

*Nano*2010, *4*, 4495-4504.
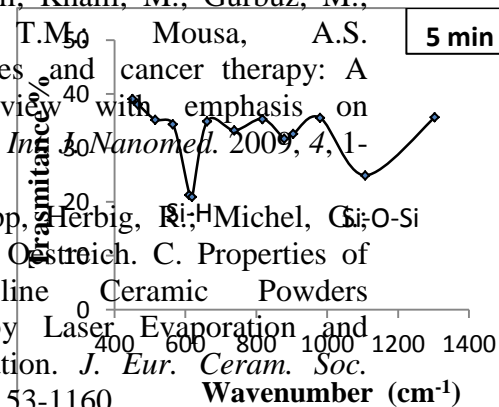
[10] C. Lee, Kim, H.; Cho, Y.; Lee, W.I. The properties of porous silicon as a therapeutic agent via the new photodynamic therapy. *J. Mater. Chem.* 2007, *17*, 2648-2653.

[11] C. Suryanarayana, Mechanical alloying and milling. *Prog. Mater Sci.* 2001, *46*, 1-184.

[12] L.D. Field, Sternhell, S.; Wilton, H.V. Mechanochemistry of some hydrocarbons. *Tetrahedron*1997, *53*, 4051-4062.

[13] R.Cioffi, De Stefano, L.; Lamanna, R.; Montagnaro, F.; Santoro, L.; Senatore, S.; Zarrelli, A.TG, FT-IR and NMR characterization of n-$C_{16}H_{34}$ contaminated alumina and silica after mechanochemical treatment. *Chemosphere* 2008, *70*, 1068-1076.

[14] L. De Stefano, Buccolieri, G.; De Luca, F.; Plescia, P. Milling effects upon quantitative determinations of chrysotile asbestos by the reference intensity ratio method. *Powder Diffr.* 2000,*15*, 26-29.

[15] P. Plescia; Gizzi, D.; Benedetti, S.; Camilucci, L.; Canizza, C.; De Simone, P.; Paglietti, F.Mechanochemical treatment to recycling asbestos-containing waste. *Waste Manage.* 2003, *23*,209-218.

[16] V.V. Boldyrev; Mechanochemical modification and synthesis of drugs. *J. Mater. Sci.* 2004, *39*,5117-5120.

[17] H.J. Fecht,. Nanostructure formation by mechanical attrition. *Nanostruct. Mater.* 1995, *6*, 33-42.